Korean J. Chem. Eng., **30**(6), 1301-1311 (2013)
DOI: 10.1007/s11814-013-0032-9

Effect of drainage channel dimensions on the performance of wave-plate mist eliminators

Mohammad Hadi Hamedi Estakhrsar and Roohollah Rafee†

Faculty of Mechanical Engineering, Semnan University, Semnan, Iran
(*Received 19 November 2012 • accepted 26 February 2013*)

Abstract−We investigated the effects of drainage channel dimensions on droplet removal efficiency and pressure drop of the gas droplet flow in a wave-plate mist eliminator. Droplet dispersion in turbulent gas flows is numerically simulated using eddy interaction model (EIM) and Eulerian-Lagrangian method. Reynolds stress transport model (RSTM) with enhanced wall treatment and shear stress transport (SST) k-ω model are used for simulating the turbulent airflow. Comparison between the numerical simulations and available experimental data shows that eddy lifetime constant (C_L) can affect the results significantly, and by selecting suitable values of the eddy lifetime constant, both turbulence models give reasonable predictions of droplet removal efficiency. Simulations of gas droplet flow in the eliminators with various drainage channel dimensions show that the drainage channel length (L_{DC}) has a greater effect on droplet removal efficiency than the drainage channel width (W_{DC}).

Key words: Numerical Simulation, Wave-plate Mist Eliminator, Drainage Channel Dimensions, Removal Efficiency, Eddy Lifetime Constant

INTRODUCTION

Wave-plate mist eliminators, also called vane or blade type separators, are widely used to remove liquid droplets from gas streams in industrial processes. For example, they are used to reduce the amount of makeup water in cooling towers by capturing the small escaping droplets.

Wave-plate function is based on droplet inertia effects. As the mixture flows through the sharp bends in narrow ducts of the eliminator, the inertia of the droplets tends to strike them on the wall. Wave-plates are constructed from thin parallel corrugated sheets mounted parallel to the flow direction. Accumulation of the droplets on the wave-plates leads to drainage of the liquid under gravity.

Performance of a mist eliminator is determined in terms of its size-dependent collection efficiency and the gas flow pressure loss across the eliminator. In a cooling tower mist eliminator, for environmental protection, the collection efficiency should be high. On the other hand, for minimization of the required fan power, the pressure loss should be low, and a compromise between these goals is required in an actual design. Computer simulations of the airflow and droplet transport and deposition in such a device can help improve the removal efficiency of the mist eliminators or reduce the gas flow pressure losses.

The droplet motion and deposition in a wave-plate mist eliminator is determined by using the Eulerian-Lagrangian method. Among the Lagrangian type models for predicting the droplet dispersion and deposition in turbulent flows, the eddy interaction model (EIM) has been applied extensively. In this model, the influence of the turbulence on the droplet dispersion is taken into account by allowing droplets to interact with eddies. Using the one-way coupling assumption, the effects of the droplets on the airflow are neglected. Eddies are characterized by their velocity, size and lifetime. The basic EIM assumes isotropic turbulence to calculate instantaneous eddy velocities from the mean flow quantities.

To improve the accuracy of the EIM, various modifications have been made. For example, the refinements proposed by Berlemont et al. [2], Zhou and Leschziner [30], Burry and Bergeles [5] are all based on Reynolds stress turbulence models and involve very time-consuming calculations.

The refinements proposed by Sommerfeld et al. [22] and Greenfield and Quarini [9], as well as Wang and James [26], are, however, based on k-ε type turbulence models.

By increasing the gas velocity, separation efficiency will rise, but as reported by Houghton and Radford [12], the maximal gas velocity is limited due to either flooding or re-entrainment of the collected liquid (See also Azzopardi and Sanaullah [1] and James et al. [14]). To overcome this problem, the introduction of drainage channels (hooks) in industrial devices has been shown to increase both separation efficiency and gas flow velocity (See McNulty et al. [17], James et al. [13] and Brunazzi et al. [3]).

Simulations for mist eliminators were carried out by Verlaan [24] and Wang and Davies [25]. Wang and James [27] showed that the calculations based on the modified k-ε model are in good agreement with experimental measurements, except for very small droplets. Galletti et al. [7] made numerical simulations using shear stress transport k-ω (SST k-ω) model and compared their results with Ghetti's [8] work. They also showed that the SST turbulence model gives better results than the standard k-ε model.

James et al. [13] studied the effect of the drainage channels on the gas flow and on the evolution of the liquid droplet distribution for a range of gas speeds, wave-plate spacing, channel sizes and inlet droplet size distributions. The ability of drainage channels to increase the droplet collection efficiency was confirmed and several features of the flow were predicted, which has implications for the design of wave-plate mist eliminators.

†To whom correspondence should be addressed.
E-mail: rafee@semnan.ac.ir

Rafee et al. [21] studied the air and droplet flows in a wave-plate mist eliminator using the Reynolds stress transport model (RSTM) with different boundary conditions. The flow and droplet trajectories in a mist eliminator were evaluated and the results were compared with the experimental data of Phillips and Deakin [19]. They showed that the RSTM with enhanced wall treatment gives better results for removal efficiency than other turbulence models.

Also, Rafee and Rahimzadeh [20] simulated the gas droplet flow inside a curved type vane separator for the examination of their developed code for gas flow simulation. They compared the code results with the experimental and numerical data from the study done by Jøsang and Melaaen [15] and Jøsang [16]. Also, the pressure loss and removal efficiency have been calculated and compared for different spacing between the plates of the vane separator. They concluded that by considering the wall reflection effects, the RSTM can predict the pressure loss and mean velocity profiles better than the RSTM without wall reflection effects. They also found the optimum plate spacing for the special curved type vane separator using numerical simulation results.

Recently, Zamora and Kaiser [29] did a numerical investigation of the collection efficiency and the pressure drop coefficient for four types of wave-plate drift eliminator with similar morphology (Belgian wave, Three-segment, L-shaped and Zig-zag), for wide ranges of the droplet size, Reynolds number and the inertial parameter. The numerical modeling was compared with numerical results of Wang and James [26,27] and Galletti et al. [7], and experimental data of Phillips and Deakin [19] and Ghetti [8]. The best results were obtained with the SST k-ω turbulence model.

The extensive use of drainage channels in the industrial practice makes it worth assessing the CFD model directly for drainage channel configurations. The present work aims partly at doing a comparison between CFD and experimental data taken in wave-plate mist eliminators equipped with drainage channels. For this purpose, the flow inside the mist eliminator was simulated numerically and the predictions were compared with the numerical results of Galletti et al. [7] and the experimental data of Ghetti [8]. Attention was also paid to the turbulent dispersion of the droplets and eddy lifetime constant. Then the effects of the drainage channel dimensions on the predicted removal efficiency and gas flow pressure drop were investigated.

GOVERNING EQUATION

1. Turbulent Airflow Field

The airflows inside the mist eliminator are typically low Reynolds number turbulent flows. It is an unfortunate fact that no single turbulence model is universally accepted as being superior for all classes of turbulent flows. The choice of a turbulence model will depend on considerations such as the physics encompassed in the flow, the established practice for a specific class of problem, the level of accuracy required, the available computational resources and the amount of time available for the simulation.

Turbulent flows are characterized by fluctuating velocity fields. These fluctuations mix transported quantities such as momentum, energy, and species concentration, and cause the transported quantities to fluctuate as well.

1-1. Reynolds Stress Transport Model (RSTM)

The basic equations of turbulent gas flow can be generalized as

Table 1. Contents of φ, Γ_φ and S_φ in general transport equation

Equation	φ	Γ_φ	S_φ
Continuity	1	0	0
Momentum	u_i	μ	$-\frac{\partial p}{\partial x_i}+\frac{\partial}{\partial x_j}(-\rho R_{ij})$
Reynolds stress	R_{ij}	$\mu+\frac{\mu_t}{\sigma_k}$	$P_{ij}+\varphi_{ij}-\varepsilon_{ij}$
TKE dissipation rate	ε	$\mu+\frac{\mu_t}{\sigma_\varepsilon}$	$\frac{\varepsilon}{k}(C_{1\varepsilon}G_k-C_{2\varepsilon}\rho\varepsilon)$

$$\frac{\partial}{\partial t}(\rho\varphi)+\frac{\partial}{\partial X_k}(\rho u_k\varphi)=\frac{\partial}{\partial X_k}\left(\Gamma_\varphi\frac{\partial\varphi}{\partial X_k}\right)+S_\varphi \tag{1}$$

where φ is the generalized dependent variable, Γ_φ, is the diffusion coefficient and S_φ is the source term. The specific parameters for φ, Γ_φ and S_φ for RSTM are listed in Table 1.

In this paper, the Reynolds stress transport model (RSTM) with enhanced wall treatment and the SST k-ω model are used to simulate the airflow. In the RSTM, the turbulent (eddy) viscosity is given as

$$\mu_t=C_\mu\rho\frac{k^2}{\varepsilon} \tag{2}$$

where k is the turbulent kinetic energy which is given by

$$k=\frac{1}{2}(R_{11}+R_{22}+R_{33}) \tag{3}$$

R_{11}, R_{22} and R_{33} are the normal Reynolds stresses. The stress production term is given as

$$P_{ij}=-\rho\left(R_{ik}\frac{\partial u_j}{\partial x_k}+R_{jk}\frac{\partial u_i}{\partial x_k}\right) \tag{4}$$

The pressure strain term, in the Reynolds stress transport equation, is completely described by Rafee et al. [20]. Also, the enhanced wall treatment option for near wall turbulence modeling is adopted in this paper (Rafee and Rahimzadeh [21]).

1-2. Shear Stress Transport k-ω (SST k-ω) Model

The shear-stress transport (SST) k-ω model was developed by Menter [18] to effectively blend the robust and accurate formulation of the k-ω model in the near-wall region with the free-stream independence of the k-ε model in the far field. In this model the definition of the turbulent viscosity is modified to account for the transport of the turbulent shear stress.

Transport equations for k and ω in SST model are as follows:

$$\frac{\partial}{\partial t}(\rho k)+\frac{\partial}{\partial x_i}(\rho k u_i)=\frac{\partial}{\partial x_j}\left(\Gamma_k\frac{\partial k}{\partial x_j}\right)+\tilde{G}_k-Y_k \tag{5}$$

and

$$\frac{\partial}{\partial t}(\rho\omega)+\frac{\partial}{\partial x_i}(\rho\omega u_i)=\frac{\partial}{\partial x_j}\left(\Gamma_\omega\frac{\partial\omega}{\partial x_j}\right)+G_\omega-Y_\omega+D_\omega \tag{6}$$

G_k represents the production of turbulence kinetic energy due to mean velocity gradient. From the exact equation for the transport of k, this term may be defined as

$$G_k = -\rho\overline{u_i' u_j'}\frac{\partial u_j}{\partial x_i} \tag{7}$$

The production of ω is given by

$$G_\omega = \alpha\frac{\omega}{k}G_k \tag{8}$$

The coefficient α is a function of k and ω and it is so calculated that in the far field regions of flow approaches to unity (α=1).

Γ_k and Γ_ω represent the effective diffusivity of k and ω, respectively, defined as

$$\Gamma_k = \mu + \frac{\mu_t}{\sigma_k} \tag{9}$$

and

$$\Gamma_\omega = \mu + \frac{\mu_t}{\sigma_\omega} \tag{10}$$

where σ_k and σ_ω are the turbulent Prandtl numbers for k and ω, respectively, μ_t is the turbulent viscosity, Y_k and Y_ω represent the dissipation of k and ω due to turbulence and D_ω is the cross diffusion term.

2. Droplet Motion and Lagrangian Tracking

It is assumed that the droplets do not affect the gas flow, which is a valid assumption for low concentrations of the droplets. The trajectory of a droplet is predicted by integrating the equation of motion of the droplet. The balance between external forces applied on the droplet with its inertia can be written as

$$\frac{du_p}{dt} = F_D(u_g - u_p) + \frac{g_x(\rho_p - \rho_g)}{\rho_p} + F_x \tag{11}$$

F_x is the acceleration due to other forces acting on the droplet. These forces include Saffman lift force and Brownian forces, and their calculation is described by Rafee et al. [20]. The authors' experiences show that the effects of these forces are negligible. The term $F_D(u_g - u_p)$ is the drag force per unit droplet mass and the coefficient of F_D is given by

$$F_D = \frac{18\mu}{\rho_p d_p^2}\frac{C_D Re_r}{24} \tag{12}$$

The droplet relaxation time (τ) is defined by

$$\tau = \frac{4\rho_p d_p}{3\rho_g C_D|\vec{u_g} - \vec{u_p}|} \tag{13}$$

Here, $\vec{u_g}$ is the gas velocity, $\vec{u_p}$ is the droplet velocity, μ is the molecular viscosity of the fluid, ρ_g is the gas density, ρ_p is the density of the droplet, and d_p is the droplet diameter. Re_r is the relative Reynolds number, which is defined by

$$Re_r = \frac{\rho_g d_p|\vec{u_p} - \vec{u_g}|}{\mu} \tag{14}$$

According to Hinds [11], the drag coefficient, C_D, is given as

$$C_D = \frac{24}{Re_p}(1 + 0.15Re_p^{0.687}) \tag{15}$$

The dispersion of droplets due to turbulence in the fluid phase can be predicted by using the stochastic tracking model. For turbulent flow, the numerical approach predicts the trajectories of droplets using the instantaneous fluid phase velocity, u, in the trajectory equations. The instantaneous gas flow velocity is given by

$$\vec{u} = \bar{u} + u' \tag{16}$$

In the discrete random walk (DRW) model, or "eddy lifetime" model, the interaction of a droplet with a succession of discrete stylized fluid phase turbulent eddies is simulated. Each eddy is characterized by a Gaussian distributed random velocity fluctuation, (u′, v′, w′) and a time scale (τ_e).

The values of u′, v′ and w′ that prevail during the lifetime of the turbulent eddy are sampled by assuming that they obey a Gaussian probability distribution, so that

$$u_i' = \zeta\sqrt{\overline{u_i'^2}} \tag{17}$$

where ζ is a normally distributed random number, and the remainder of the right-hand side is the local rms value of the velocity fluctuations. For the SST k-ω model, since the kinetic energy of turbulence is known at each point in the flow, these values of the rms fluctuating components can be defined (assuming isotropy) as

$$\sqrt{\overline{u'^2}} = \sqrt{\overline{v'^2}} = \sqrt{\overline{w'^2}} = \sqrt{\frac{2k}{3}} \tag{18}$$

When the RSTM is used, anisotropy of the stresses is included in the derivation of the velocity fluctuations:

$$u' = \zeta\sqrt{\overline{u'^2}} \tag{19a}$$

$$v' = \zeta\sqrt{\overline{v'^2}} \tag{19b}$$

$$w' = \zeta\sqrt{\overline{w'^2}} \tag{19c}$$

In the eddy interaction model (EIM) it is assumed that the droplets encounter discrete eddies characterized by a length scale that is given by

$$L_e = 0.164\frac{k^{\frac{3}{2}}}{\varepsilon} \tag{20}$$

The fluid Lagrangian integral time scale, T_L time scale can be approximated as

$$T_L = C_L\frac{k}{\varepsilon} \tag{21}$$

The value of C_L is the eddy lifetime constant, and in the different situations this parameter has various values. According to Tian and Ahmadi [23], C_L is in the range of 0.2-0.96. This study shows that the results of numerical simulation depend on this value. Also, by adjusting the value of C_L for different Reynolds numbers, better predictions can be achieved. For k-ω models, $\omega = \varepsilon/k$ must be substituted into Eq. (21).

The droplet eddy crossing time is defined as

$$t_{cross} = -\tau\ln\left[1 - \left(\frac{L_e}{\tau|\vec{u_g} - \vec{u_p}|}\right)\right] \tag{22}$$

Where τ is the droplet relaxation time (see Eq. (13)) and L_e is the

eddy length scale.

The above expression is valid only if $L_e/(\tau|\vec{u}_g-\vec{u}_p|)$. If this inequality does not hold, the droplet is "captured", and t_{cross} is set equal to characteristics eddy lifetime. The characteristic lifetime of the eddy is defined either as a constant ($\tau_e=2T_L$) or as a random variation about T_L

$$\tau_e=-T_L \log(r) \quad (23)$$

where r is a uniform random number between 0 and 1. In varied EIM the start of an eddy interaction, the random number ζ is sampled and is kept constant during the droplet-eddy interaction as in constant EIM. However, both the mean velocity and the fluctuating velocity in Eq. (19) are changed when a droplet crosses a control volume boundary as are the eddy lifetime and eddy length scale. The authors use the standard EIM, but the option of random calcu-

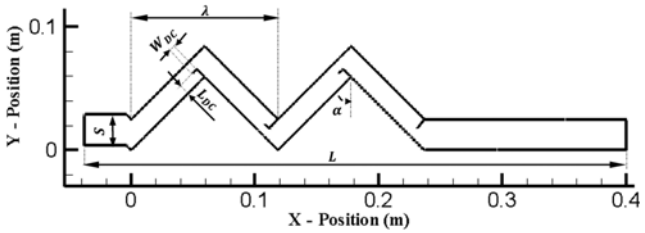

Fig. 1. Geometry of the wave plate mist eliminator.

Table 2. Geometrical details of wave-plate mist eliminator

L_{CD} (mm)	W_{DC} (mm)	L (mm)	α	S (mm)	λ (mm)
8.6	4.3	437.5	45°	25	118.5

Table 3. Details of different types of drainage channels

Type of drainage channel	L_i	W_i
Type 1	$L_1=L_{DC}$	$W_1=W_{DC}$
Type 2	$L_2=0.5L_{DC}$	$W_2=W_{DC}$
Type 3	$L_3=1.25L_{DC}$	$W_3=W_{DC}$
Type 4	$L_4=L_{DC}$	$W_4=0.5W_{DC}$
Type 5	$L_5=L_{DC}$	$W_5=1.5W_{DC}$
Type 6	$L_6=0$	$W_6=0$

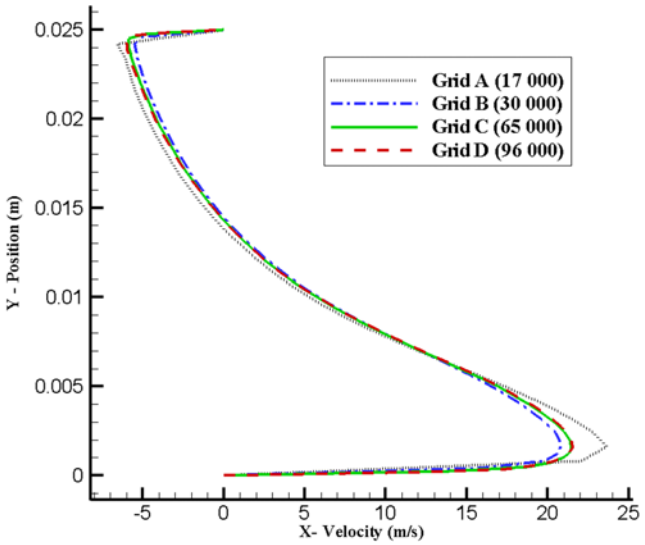

Fig. 2. u-Component velocity profile after the last bend of mist eliminator (x=0.3 m).

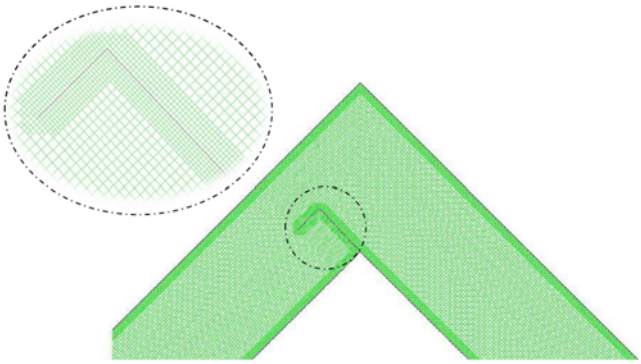

Fig. 3. Details of the generated mesh at the bends.

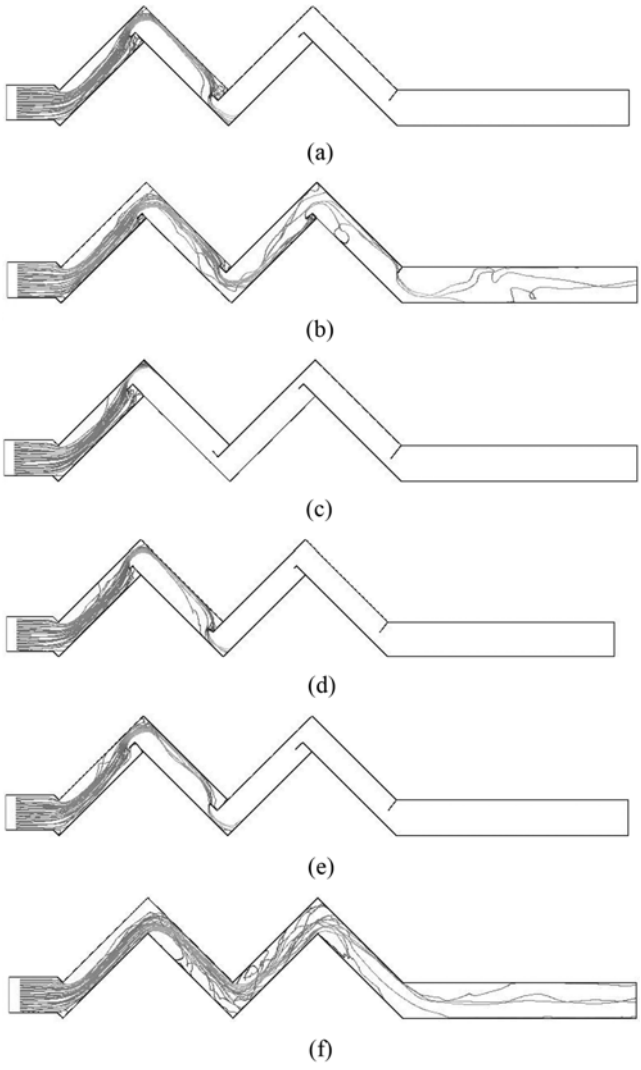

Fig. 4. Trajectories of the droplets in the wave plate mist eliminator with six different types of drainage channel: (a) *type 1*, (b) *type 2*, (c) *type 3*, (d) *type 4*, (e) *type 5* and (f) *type* 6.

lation of τ_e is used for calculation in this paper. The options of random calculation of τ_e yield a more realistic description of the correlation function, and it is used for calculation in this paper.

MESH GENERATION

In this study the flow inside a wave-plate mist eliminator with various drainage channel dimensions is considered. The geometry of the problem is shown in Fig. 1 and dimensions of wave-plate and drainage channel are given in Table 2.

To study the effects of variations in drainage channel dimensions, the flow through six different geometries was simulated. Dimensions of the drainage channels are given in Table 3. *Type 6* is an eliminator without drainage channel.

Several grids with total number of 17,000, 30,000, 65,000 and 96,000 quadrilateral cells were generated and used for simulation. Fig. 2 shows the u-velocity component profile after the last bend (at x=0.3 m) of original drift eliminator (type 1) with inlet gas velocity of 5 m/s. It can be seen that the grid independent solution is obtained by grid C (65,000 quadrilateral cells).

Interval size for grid D is 0.0004 m. Near the walls, finer meshes with the element size of 1.33×10^{-4} m were generated. Details of the mesh at the bends are shown in Fig. 3.

NUMERICAL SIMULATION

Reynolds stress transport model (RSTM) with enhanced wall treatment and shear stress transport model (SST) k-ω model are used to simulate the steady airflow field in the wave plate mist eliminator. The results are compared with the available experimental data. All simulations were performed using Fluent 6.3.26 software.

Airflows with density of ρ=1.225 kg/m^3 and viscosity of μ= 1.789×10^{-5} Ns/m^2 and with the bulk velocities in the range of 2 to 5 m/s were simulated. The corresponding to Reynolds numbers are in the range of 6 847-17 118. Turbulence intensity of 5% and hydraulic diameter of were assumed for calculation of turbulence quanti-

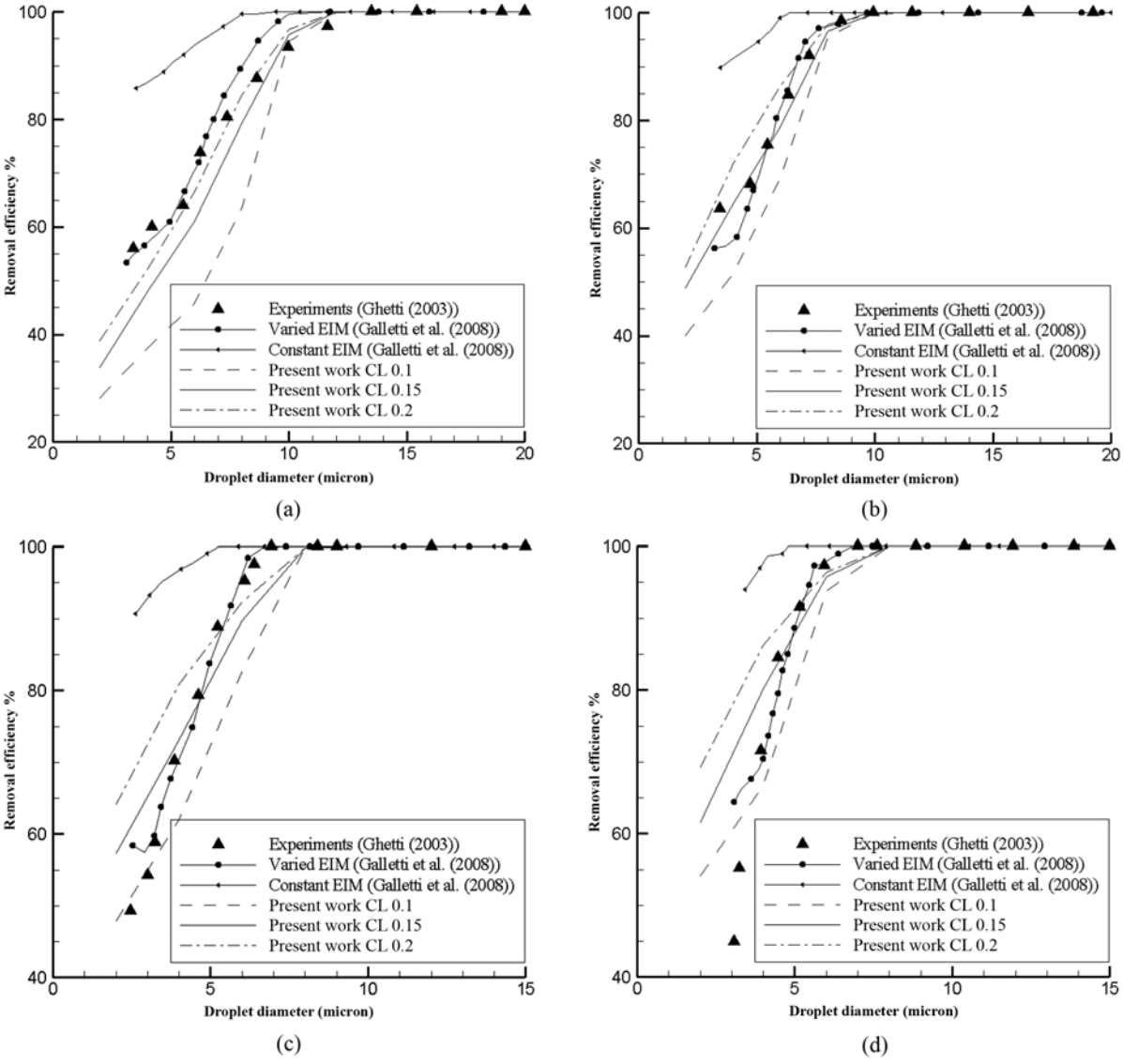

Fig. 5. Comparison between predicted droplet removal efficiency and experimental data for *type 1* at different gas velocities (a) U_g=2 m/s, (b) U_g=3 m/s, (c) U_g=4 m/s and (d) U_g=5 m/s. Simulations with SST k-ω model.

ties at the inlet.

The finite volume method (FVM) was adopted for discretization of the governing equations. For pressure velocity coupling the 'SIMPLE' algorithm was used. The spatial discretization of convective terms was performed using upwind scheme. The diffusion terms in the governing equation are central-differenced and are always second-order accurate. The residual of 10^{-5} is selected as the convergence criterion for termination of the solution procedure of the gas flow equations. The steadiness of the residuals with iterations was checked for all of the simulations.

As mentioned before, the effects of the droplets on the gaseous phase were not taken into account. The incoming sprayed water was simulated by assuming a high enough number of injections placed at the inlet section of domain.

For each droplet size, 1500 water droplets were injected at the inlet of the mist eliminator. The mean droplet sizes were in the range of 1-20 μm. The velocity of the droplets at the inlet is equal to gaseous phase velocity. Droplet motion was simulated with three different time scale constants (C_L=0.1, 0.15 and 0.2) for turbulent dispersion. Droplet motion equations were solved using the high order Runge-Kutta scheme.

According to Zamora and Kaiser [29] the outlet pressure is set to be equal to ambient pressure. Assuming that the flow discharged in a jet-like manner to the ambient at exit, the streamwise variations of all properties were neglected. The simulation was isothermal and two-dimensional and all the walls are considered adiabatic. At walls, no-slip boundary conditions were imposed for gas velocity components. It is assumed that when a droplet reaches the wall, it is deposited on the wall and removed from the gas stream.

Trajectories of the droplets in the gas flow with the bulk velocity of 5 m/s are shown for six different types of drainage channels in Fig. 4. These simulations were performed by using RSTM. Mean droplet sizes are equal for all simulations in this figure. As can be seen, some droplets can escape from the eliminator *Type 6* and *Type 2*. Therefore, these types have lower removal efficiency than the other types.

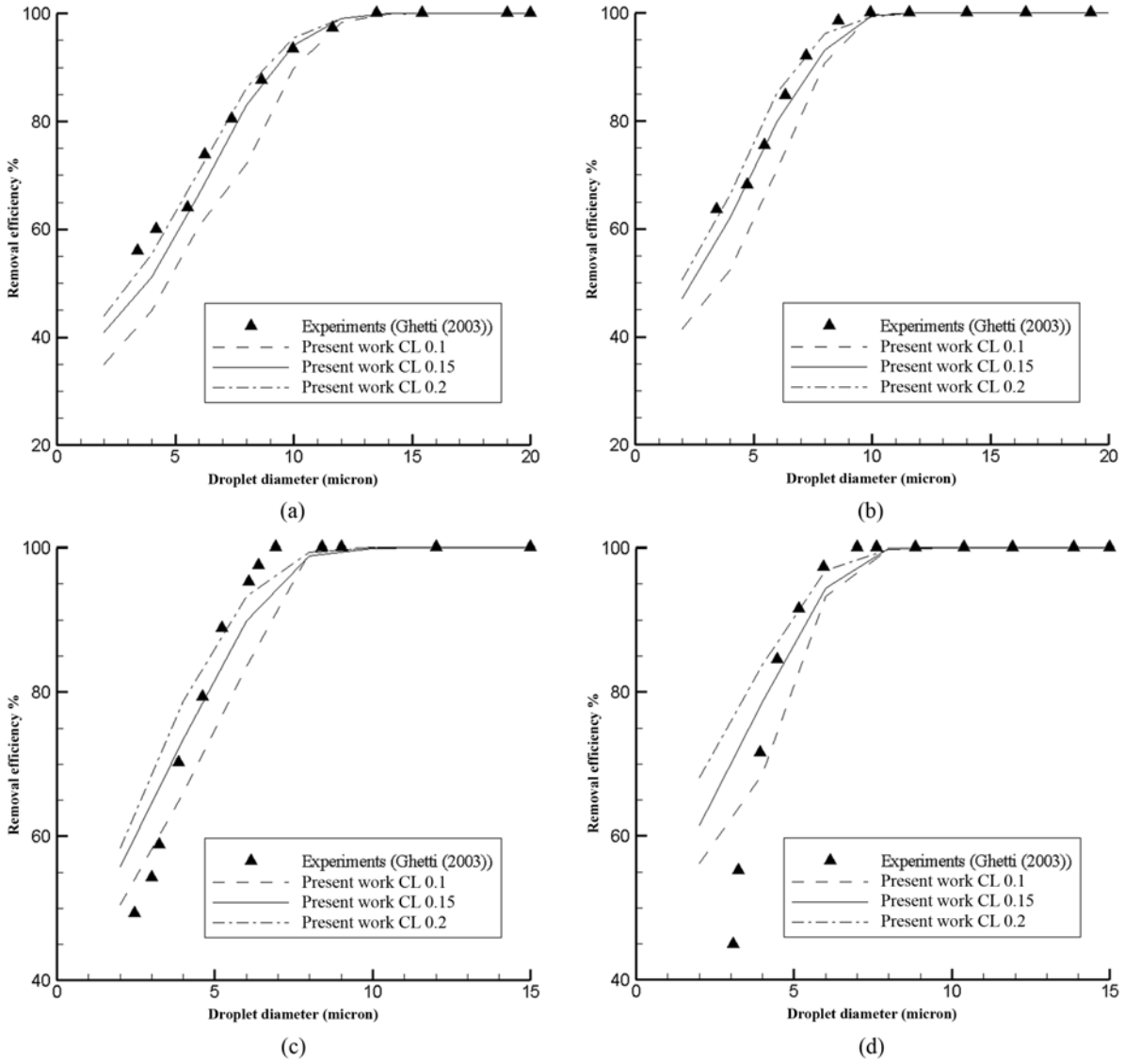

Fig. 6. Comparison between predicted droplet removal efficiency and experimental data for *type 1* at different gas velocities (a) U_g=2 m/s, (b) U_g=3 m/s, (c) U_g=4 m/s and (d) U_g=5 m/s. Simulations with RSTM.

RESULTS AND DISCUSSION

1. Removal Efficiency

There is an analytical formula for calculating the removal efficiency in a simple zig-zag mist eliminator without drainage channel (See e.g. Calvert et al. [6] and Bürkholz [4]). However, this formula is not applicable for eliminators having drainage channels. The droplet collection efficiency (or droplet removal efficiency) is defined as

$$\eta = \frac{\text{mass of removed droplets}}{\text{mass of entering droplets}} \tag{24}$$

The numerical results were compared with experimental data of Ghetti [8] and the numerical results of Galletti et al. [7], in order to achieve an appropriate validation of the stated numerical model. Ghetti [8] investigated the performance of different types of commercial wave-plate mist eliminators operated at atmospheric working conditions with horizontal gas flow. Type 1 geometry corresponds to Ghetti's [8] experiments.

Fig. 5 compares the predicted efficiencies obtained with SST k-ω model with the previous experimental and numerical data. Results are presented for three different values of eddy lifetime constant (C_L=0.1, 0.15, 0.2). The first geometry (*Type 1*) is considered in these simulations and the bulk gas velocities are in the range of 2 to 5 m/s. As shown, the predicted results depend on the eddy lifetime constant (C_L). When the SST k-ω model is used, there is no constant optimum value of C_L for all range of the gas velocity.

For SST k-ω model, at the gas velocity of 2 m/s, C_L=0.2 gives the best results. However, for gas velocities in the range of 3-5 m/s, C_L=0.15 is the best choice.

When RSTM is used (See Figs. 6(a) to 6(d)), C_L=0.2 and C_L= 0.15 give better predictions in the range of 2 to 5 m/s. Previously, Zamora and Kaiser [29] reported that the EIM predictions are sensitive to values of C_L. In this paper, we found the best choice for C_L, and then studied the effects of changes in drainage channel dimensions on performance of the mist eliminator.

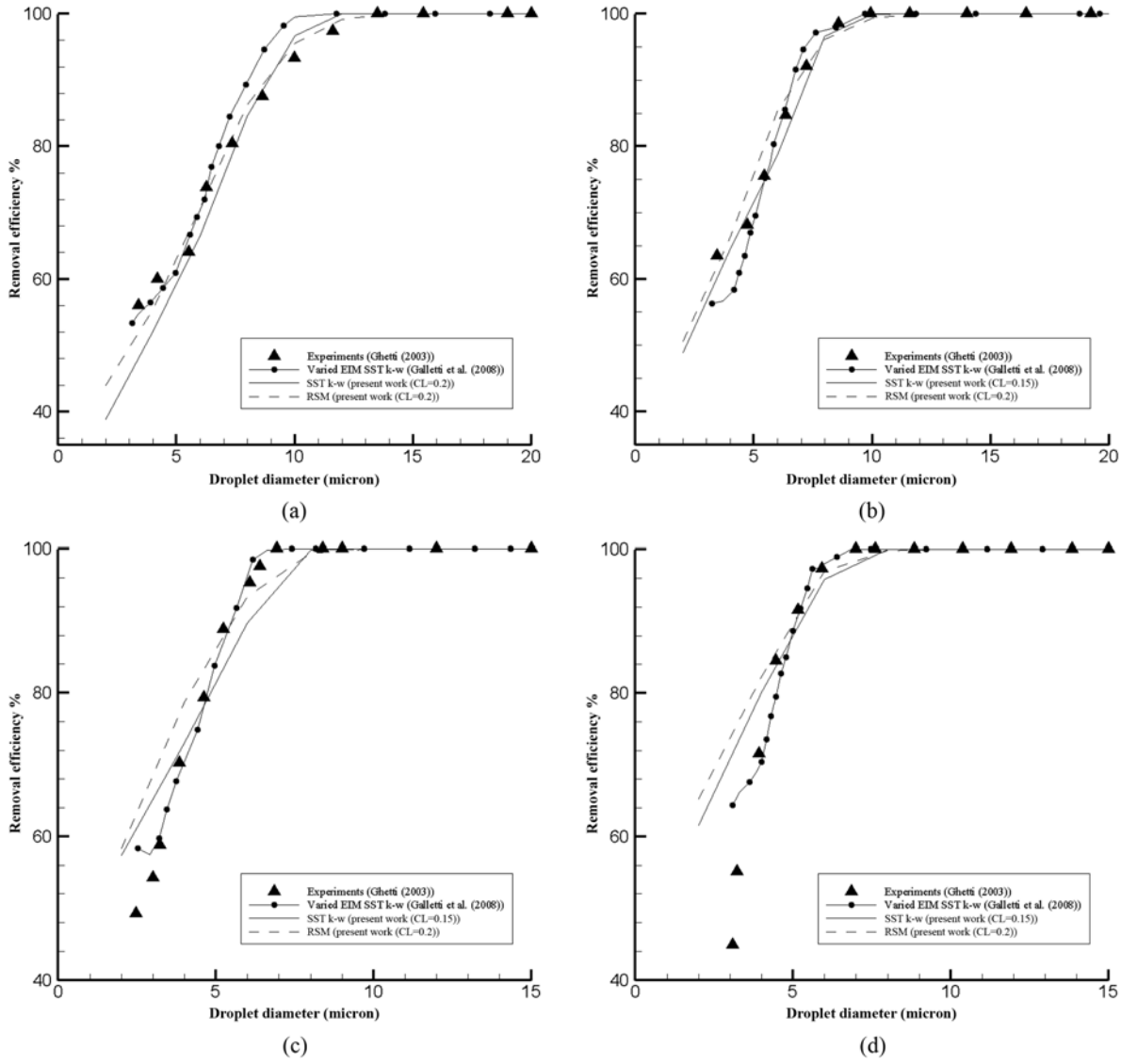

Fig. 7. Comparison of the obtained results with available experimental and numerical data for different gas velocities (a) U_g=2 m/s, (b) U_g= 3 m/s, (c) U_g=4 m/s and (d) U_g=5 m/s.

Fig. 7 compares the best results obtained with SST k-ω model and RSTM with the previous experimental and numerical data for different gas velocities. Both turbulence models give reasonable predictions in these cases.

Influences of the variations in drainage channel length (L_{DC}) on the predicted removal efficiency of the eliminator are shown in Fig. 8.

These results are presented for constant value of the drainage channel width (W_{DC}=4.3 mm) and for RSTM. It can be concluded that the eliminators with higher drainage channel length have higher removal efficiencies than those that have channels with shorter length. For example, at the gas velocity of 2 m/s and for L_{DC}=8.6 mm, if the channel length increases by 25%, the removal efficiency of 6 μm droplets will increase by 28% (See Fig. 8(a)).

The SST k-ω model predictions for Type 2 in some droplet sizes are not reasonable. In some droplet sizes, this model predicts higher removal efficiency for Type 6 (without drainage channel) than those for Type 2. Note that the turbulent flows near the walls are naturally anisotropic. Therefore, the obtained rms fluctuating components using SST k-ω model are not very accurate. These fluctuating velocities can affect the path of the droplets in the range of interest of the sizes. The existence of the drainage channel walls gives higher anisotropy in turbulent gas flow, and it seems that the RSTM gives more reasonable prediction in these cases.

The effects of the variations in drainage channel width (W_{DC}) on the eliminator efficiency are illustrated in Fig. 9. The results are shown for different types of drainage channel (*Type 1* (W_1=W_{DC}=4.3 mm), *Type 4* (W_4=0.5W_{DC}), *Type 5* (W_5=1.5W_{DC}) and *Type 6* (W_6=0)). This figure shows that the size of the drainage channel width is not a very important parameter in eliminator efficiency. However, if the drainage channel is removed (*Type 6*), the efficiency will decrease significantly.

The probability of re-entrainment should be checked. The worst condition occurs for *Type 6* (without drainage channel). For the gas flow velocity of 5 m/s and mean droplet size of 20 μm (where removal efficiency is 100%), the maximum deposition occurs on the upper wall after the first bend. For liquid mass loading of 0.015 kg/

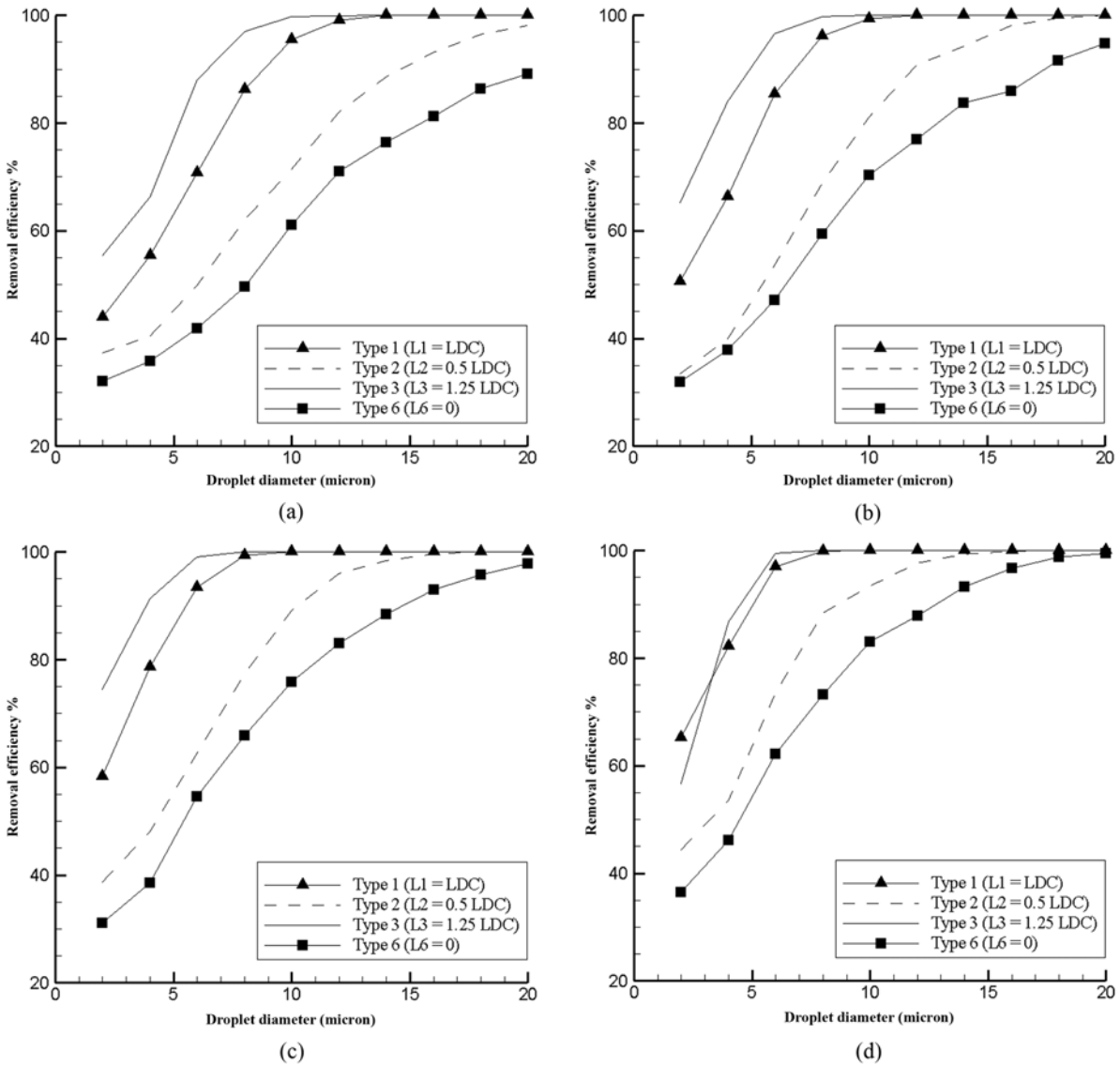

Fig. 8. Predicted droplet removal efficiency for different drainage channel lengths (*type 1* (L_1=L_{DC}), *type 2* (L_2=0.5L_{DC}), *type 3* (L_3=1.25L_{DC}) and *type 6* (L_6=0)) for different gas velocities: (a) U_g=2 m/s, (b) U_g=3 m/s, (c) U_g=4 m/s and (d) U_g=5 m/s. Simulations with RSTM.

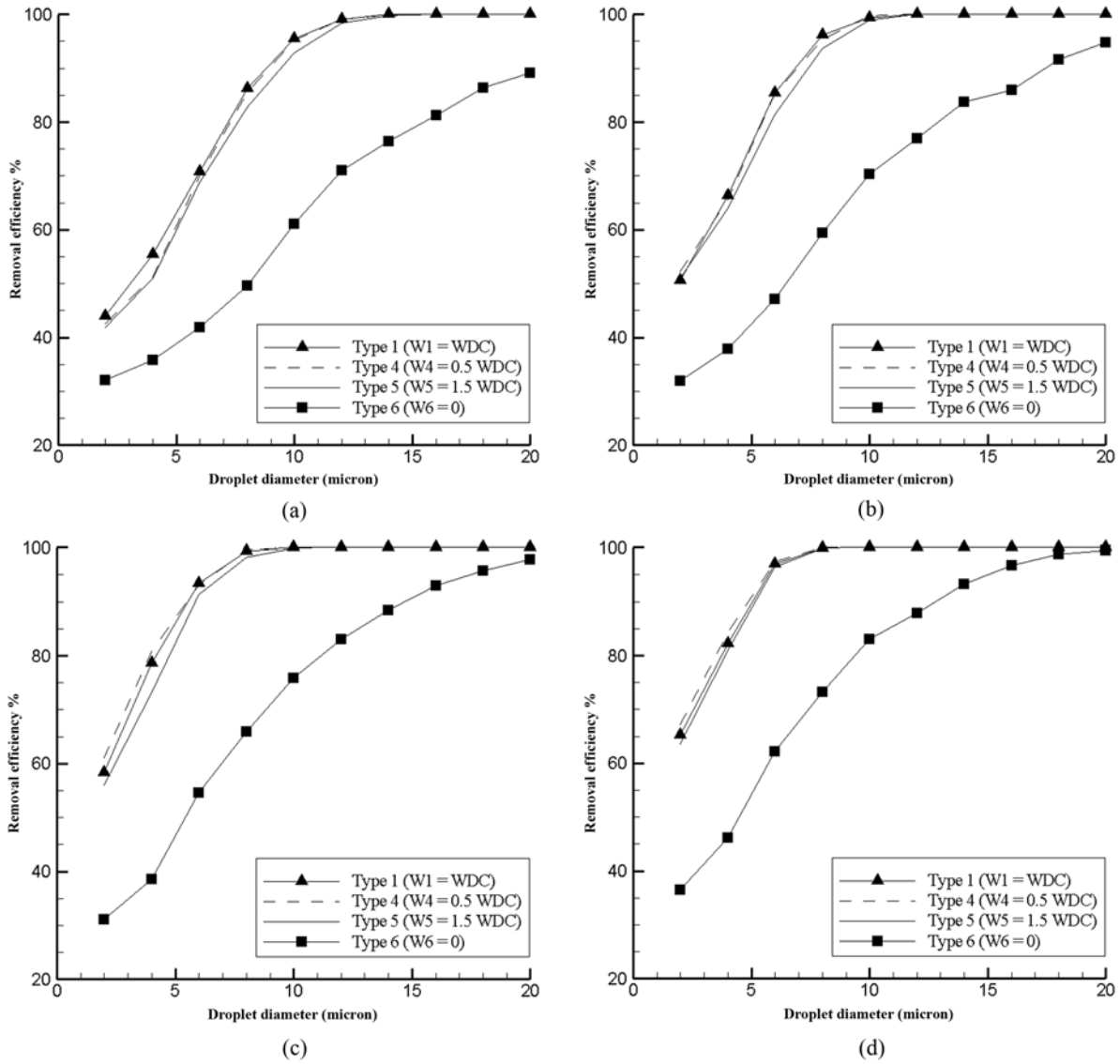

Fig. 9. Predicted droplet removal efficiency for different drainage channel widths (*type 1* (W_1=W_{DC}), *type 4* (W_4=0.5W_{DC}), *type 5* (W_5= 1.5W_{DC}) and *type 6* (W_6=0)) for different gas velocities: (a) U_g=2 m/s, (b) U_g=3 m/s, (c) U_g=4 m/s and (d) U_g=5 m/s. Simulations with RSTM.

sec (the ratio of the mass flow rate of the droplets to the air flow should be less than 0.1 to assume that the presence of the droplets does not affect the gas flow), the mean rate of the droplet deposition is 0.0083 kg/sec. Azzopardi and Sanaullah [1] present the critical gas velocity for a bend at which the re-entrainment will occur. For the mentioned conditions, liquid film Reynolds number ($4\dot{m}_{liquid}$ / $b\mu_l$) will be 33.2, and according to the results of Azzopardi and Sanaullah's [1] study, the minimum critical gas flow velocity will be 7.5 m/s. This guarantees that the effect of re-entrainment is negligible.

2. Pressure Drop

According to Wilkinson [28], as the gas flows through the channels in a wave-plate, recirculation zones form downstream of the each bend on the convex side. Each recirculation zone forms a blockage in the channel, reducing its effective width for the main flow. This causes acceleration of the bulk flow passing the recirculation zone, leading to a reduction in the static pressure according to Bernoulli's equation. As the flow decelerates and reattaches downstream of the recirculation zone, there is some recovery of pressure, but this is not complete due to energy dissipation, particularly in the recirculation zone.

Pressure drops in the wave plate mist eliminator for various drainage channels are compared in Figs. 10 and 11. Fig. 10 shows the effects of drainage channel length (L_{DC}) on the mist eliminator pressure drop. As illustrated, by increasing the channel length, there is an augmentation in gas flow pressure drop because the gas flow passage will be more blocked. For an eliminator with small drainage channel length (*Type 2*) the pressure drop is almost equal to the eliminator without drainage channel (*Type 6*) (See Fig. 10), but the removal efficiency is higher (See Fig. 8).

The change in width of the channel has little effect on the gas flow pressure drop (see Fig. 11). In fact, by increasing the channel width, the blockage in the gas flow passage does not change significantly. Also, for eliminators with drainage channel, by increasing the channel width the pressure loss decreases.

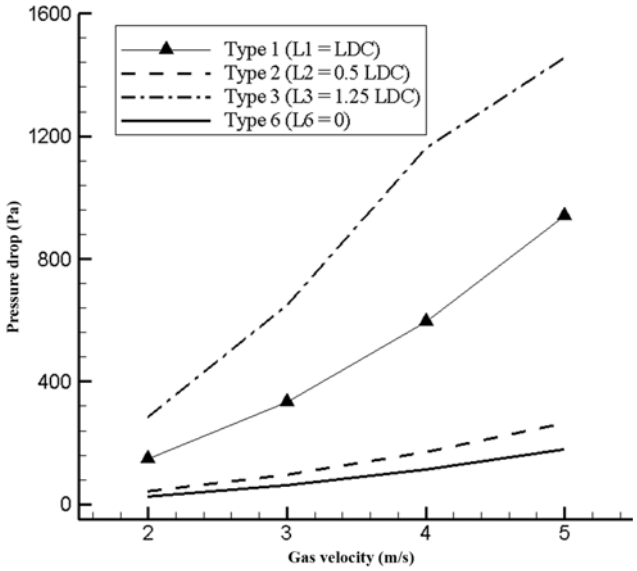

Fig. 10. Effects of drainage channel length on the mist eliminator pressure drop: Simulations with RSTM.

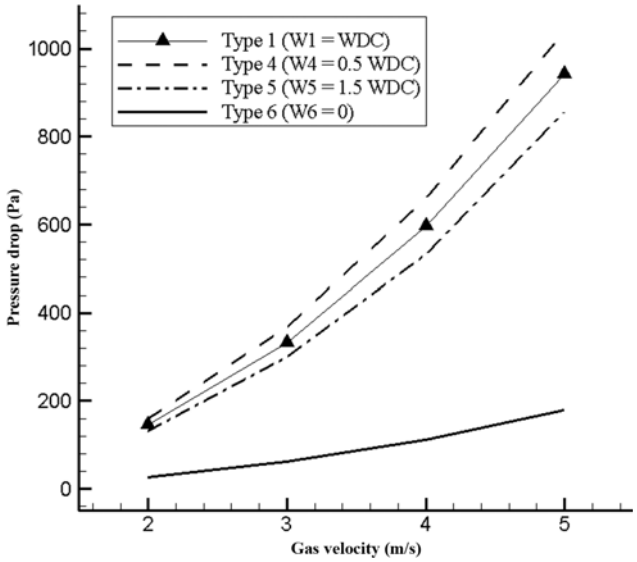

Fig. 11. Effects of drainage channel width on the mist eliminator pressure drop: Simulations with RSTM.

CONCLUSIONS

Air droplet flow has been numerically studied in wave-plate mist eliminators with various drainage channel dimensions. First, for validation of the numerical method, the predicted removal efficiencies of the mist eliminator were compared with available experimental and numerical data of Ghetti [8] and Galletti et al. [7]. Then the effects of drainage channel dimensions on the droplet removal efficiency and the gas flow pressure loss were investigated numerically.

Some important findings from the air droplet flow simulations are:

- Comparison between the numerical and experimental data for removal efficiency shows that the results depend on the eddy lifetime constant (C_L). For both turbulence models (SST k-ω and RSTM) C_L=0.15 and C_L=0.2 give the best predictions.
- Changing the drainage channel length can change the droplet collection efficiency of the eliminators significantly. For example at the gas velocity of 2 m/s if the channel length increases by 25%, the removal efficiency of 6 μm droplets will increase by 28% (See Fig. 8(a)).
- The length of the drainage channel (L_{DC}) is a key parameter for determining the removal efficiency. However, the drainage channel width (W_{DC}) is not a significant parameter in the range of sizes we investigated (See Fig. 9).
- The results show that by increasing the length of drainage channel, the gas flow passage will be narrower and more pressure losses will occur in the gas stream.
- For the mentioned range, by increasing the channel width, in most cases the removal efficiency and pressure loss will decrease.
- For an eliminator with small drainage channel length (*Type 2*) the pressure drop is almost equal to the eliminator without drainage channel (*Type 6*) (See Fig. 10), but the removal efficiency is higher (See Fig. 8).

NOMENCLATURE

b : depth of the mist eliminator [m]
C_D : drag coefficient [-]
C_L : eddy lifetime constant [-]
d_p : droplet diameter [m]
D_ω : cross diffusion terms [kg/m^{3}s^2]
F_D : coefficient in drag force acceleration [1/s]
F_x : additional acceleration [m/s^2]
G_k : production of turbulence kinetic energy [kg/ms^3]
G_ω : production of ω [kg/m^{3}s^2]
k : turbulent kinetic energy [m^2/s^2]
L : length of wave plate [mm]
L_{DC} : length of drainage channel [mm]
W_{DC} : width of drainage channel [mm]
L_e : eddy length scale [m]
$\dot{m}_{liquid}$: liquid film mass flow rate [kg/s]
n : number of bend [-]
Re_g : gas Reynolds number [-]
Re_p : droplet Reynolds number [-]
Re_r : relative Reynolds number [-]
R_{ij} : Reynolds stress tensor [m^2/s^2]
S : channel width [mm]
S_φ : source term in transport equation
T : integral time scale [s]
t : time [s]
t_{cross} : eddy crossing time [s]
$\bar{u}$: average gas velocity [m/s]
u′ : gas fluctuating velocity component [m/s]
u_p : droplet velocity component [m/s]
Y_k : dissipation of kinetic energy [kg/ms^3]
Y_ω : dissipation of ω [kg/m^{3}s^2]
Γ_k : effective diffusivity of kinetic energy [kg/ms]
Γ_ω : effective diffusivity of ω [kg/ms]
Γ_φ : diffusion coefficient in transport equation
η : droplet removal efficiency [%]
α : bend angel [deg]

ε : dissipation rate [m^2/s^3]
λ : bend wavelength [mm]
μ_l : liquid film dynamic viscosity [kg/ms]
μ_t : turbulent dynamic viscosity [kg/ms]
ρ_g : gas density [kg/m^3]
ρ_p : droplet density [kg/m^3]
σ_k : turbulent Prandtl numbers for [-]
σ_ω : turbulent Prandtl numbers for [-]
τ_p : droplet relaxation time [s]
φ : general variable in transport equation

REFERENCES

1. B. J. Azzopardi and K. S. Sanaullah, *Chem. Eng. Sci*., **57**, 3557 (2002).
2. A. Berlemont, P. Desjonqueres and G. Gouesbet, *Int. J. Multiphase Flow*, **16**, 19 (1990).
3. E. Brunazzi, S. Ghetti, C. Merello and A. Paglianti, in *Proceedings of* Convegno Gricu 625 (2004).
4. A. Burkholz, *Droplet separation*, VCH Publishers, New York, USA (1989).
5. D. Burry and G. Bergeles, *Int. J. Multiphase Flow*, **19**, 65 (1993).
6. S. Calvert, I. L. Jashnani and S. Yung, *J. Air Pollution Control Association*, **24**, 967 (1974).
7. Ch. Galletti, E. Brunazzi and L. Tognotti, *Chem. Eng. Sci*., **63**, 5639 (2008).
8. S. Ghetti, *M. Sc. Thesis*, University of Pisa, Pisa, Italy (in Italian) (2003).
9. C. Greenfeld and G. Quarini, *ASME fluids engineering division summer meeting*, June 22 (1997).
10. K. Hanjalic and B. E. Launder, *J. Fluid Mechnol*., **51**, 301 (1972).
11. W. C. Hinds, *Aerosol technology: Properties, behavior, and measurement of airborne particles*, Wiley, New York (1982).
12. H. G. Houghton and W. H. Radford, *Transactions of the American Institution of Chemical Engineers*, **35**, 427 (1939).
13. P. W. James, Y. Wang, B. J. Azzopardi and J. P. Hughes, *Chem. Eng. Res. Des*., **81**, 639 (2003).
14. P. W. James, B. J. Azzopardi, Y. Wang and J. P. Hughes, *Chem. Eng. Res. Des*., **83**, 469 (2005).
15. A. I. Jøsang and M. Chr. Melaaen, in *42nd Scandinavian Conference on Simulation and Modeling Porsgrunn*, Norway, October 8 (2001).
16. A. I. Jøsang, *Ph.D. Thesis*, Dep. of Technol. (HiT-TF), Telemark Univ. Coll., Norway (2002).
17. K. J. McNulty, J. P. Monat and O. V. Hansen, *Chem. Eng. Progress*, **83**, 48 (1987).
18. F. R. Menter, *AIAA J.*, **32**, 1598 (1994).
19. H. Phillips and A. W. Deakin, in *4th Annual Meeting of the Aerosol Society Loughborough*, UK (1990).
20. R. Rafee, H. Rahimzadeh and G. Ahmadi, *Chem. Eng. Res. Des*., **88**, 1393 (2010).
21. R. Rafee and H. Rahimzadeh, *Iran J. Chem. Chem. Eng*., **29**, 97 (2010).
22. M. Sommerfeld, G. Kohnen and M. Ruger, in *9th Symp. Turbulent Shear Flows*, Kyoto, Japan, August 16 (1993).
23. L. Tian and G. Ahmadi, *J. Aerosol Sci*., **38**, 377 (2007).
24. C. C. J. Verlaan, *Ph.D. Thesis*, Delft University of Technology, Delft, the Netherlands (1991).
25. Y. Wang and G. A. Davies, *IChemE Part A: Chem. Eng. Res. Des*., **74**, 232 (1996).
26. Y. Wang and P. W. James, *Chem. Eng. Res. Des*., **76**, 980 (1998).
27. Y. Wang and P. W. James, *Chem. Eng. Res. Des*., **77**, 692 (1999).
28. D. Wilkinson, *IMechE Part E: Proc. Instn. Mech. Eng*., **213**, 265 (1999).
29. B. Zamora and A. S. Kaiser, *Chem. Eng. Sci*., **66**, 1232 (2011).
30. Q. Zhou and M. A. Leschziner, in *8th Symp. Turbulent Shear Flows*, Technical University of Munich, Germany, September (1991).